DOI: 10.1002/ejic.200900594

Syntheses, Crystal Structures, and Spectroscopic Studies of Aromatic Ester Derivatives of Hexamolybdate

Qiang Li,[a] Panchao Yin,[b] Lu Shi,[b] and Yongge Wei*[b]

Keywords: Polyoxometalates / Hexamolybdate / Organic and inorganic hybrids / Drug delivery / Hydrogen bonds

Two new hybrids of local anesthetic analogs and polyoxometalates $\{(Bu_4N)_2[Mo_6O_{18}NC_6H_4COOCH_3]$ (**1**) and $(Bu_4N)_2[Mo_6O_{18}NC_6H_4COOC_2H_5]$ (**2**)$\}$ have been prepared in high purity and moderate yields using the easy reaction route of $[\alpha\text{-}Mo_8O_{26}]^{4-}$ with corresponding aromatic amine hydrochlorides in the presence of a *N,N′*-dicyclohexylcarbodiimide (DCC), and have been characterized by ^{1}H NMR, IR, UV/Vis, ESI-MS, and single-crystal X-ray diffraction study. Compound **1** crystallizes in the triclinic space group $P\bar{1}$ with dimer structure, while Compound **2** crystallizes in the monoclinic space group $P2_1/n$ with dimer and chain structure. These two hybrids have the typical Mo≡N triple bond that links a phenylimido group in local anesthetic analogs to the Mo atom of a hexamolybdate cluster. Because the formed Mo≡N bond is not stable in basic solution, this property is useful and could be developed as a novel controlled-release technology for drug delivery.

Introduction

As a large type of metal oxide complex based on early transitional metals, polyoxometalates (POMs) have attracted a lot of attention in the last years because of their varied potential applications in catalysis, supramolecular inorganic chemistry, electron transfer reaction, crystal engineering, biological chemistry, and pharmacy.[1–6] In order for the properties of POMs to be more tunable and potential applications to be more realizable, appropriate modifications are introduced into POM anions.[7,8] Especially, organically modified POMs are applied to construct frameworks for catalysis immobilization,[9] introduce anchor positions and organic functional groups,[10] design nonlinear optics materials,[11] compounds with special biological activity,[12] and to form amphiphathic molecules.[13]

To the best of our knowledge, the introduction of organic functional groups to POM parent anions is one of the most important topics in organic modification of POMs. Because of the introduction of amino groups into Anderson-type POMs, pyrene units and long alkyl chains can be attached to the Anderson anions through Schiff base reaction and amide reaction.[14,15] Cronin went on to study the special self-assembly behavior of such derivatives.[13–15] On the basis of the same reaction and parent anions, Hasenknopf et al. grafted pyridine to Anderson anions and investigated the coordination chemistry of the products.[16,17] The amine groups can also replace halogen atoms through nucleophilic reaction; Hill et al.[10] anchored carboxyl groups onto the surface of Lindqvist-type POMs and the product was used to construct a 3-D framework on the basis of the coordination effect of carboxyl. Furthermore, Cronin et al.[18] discovered that functional groups anchored onto Dawson-type POMs can lead to protein-sized supramolecular assemblies, which was monitored by ESI. Maatta et al.[19] was the first to graft olefin groups to hexamolybdate and then the monomer obtained was polymerized. In recent years, we have tried to link varied functional groups to hexamolybdate and have studied their properties using a DCC-catalyzed hexamolybdate organic imido reaction protocol. Bromide and iodine derivatives of hexamolybdate were studied with the Suzugaki and Heck reactions.[20,21] The esterification reactions and hydrogen-bonding assembly of hydroxy derivatives were studied.[22,23] Derivatives containing fluorin were found to be good herbicides.[24,25]

In organic chemistry, the ester group can be applied in ester exchange, hydrolyzation, and aminating reactions.[26] Also the ester group can have special biological activity. As a common ingredient in sunburn remedies and first-aid creams, benzocaine, which is the ligand of compound **2**, is a topical anesthetic—it numbs the nerve endings near the surface of the skin on application. It is used to reduce pain or discomfort caused by minor skin irritation, sore throat, sunburn, teething pain, vaginal or rectal irritation, ingrown toenails, hemorrhoids, and many other sources of minor pain on the surface of the body. Benzocaine is also used to numb the skin or surfaces inside the mouth, nose, throat, vagina, or rectum to lessen the pain of inserting a medical instrument such as a tube or speculum.[27] Benzocaine is an

[a] Department of Chemistry, College of Science of Beijing Forestry University,
Beijing 100083, P. R. China
[b] Department of Chemistry, Tsinghua University,
Beijing 100084, P. R. China
E-mail: yonggewei@mail.tsinghua.edu.cn

ester-type anesthetic, which contains an amino group, and based on our approach to functionalize α-octamolybdate $[\alpha\text{-}Mo_8O_{26}]^{4-}$ with aromatic amines, a new hybrid will be fabricated.[28] Because the organic benzocaine and the inorganic POMs can combine covalently, the resulting hybrid materials will surely differ from their parents, and some new properties will also be obtained. For example, the formed Mo≡N bond is not stable in basic solution, and upon decomposition of the resulting hybrid, benzocaine will be released. Such a property could be developed as a novel controlled-release technology for drug delivery.

In this paper, we report on the detailed syntheses and structural characterization of two ester-type anesthetics functionalized by arylimido derivatives of hexamolybdate, i.e. $(Bu_4N)_2[Mo_6O_{18}NC_6H_4COOCH_3]$ (**1**) and $(Bu_4N)_2[Mo_6O_{18}NC_6H_4COOC_2H_5]$ (**2**). Results from UV/Vis spectroscopy, ^{1}H NMR, IR spectroscopy, and X-ray crystallography are combined to provide a detailed description of these two ester functionalized polyoxometalates.

Results and Discussion

Synthesis

To investigate the properties of the ester-type anesthetic derivatives of polyoxometalates, two novel monofunctionalized organoimido derivatives of hexamolybdate incorporating ester groups were synthesized with the DCC aromatic amine hydrochloride method, which had been reported in our previous work.[28] Compared with the other reported analogs, the reaction of methyl *p*-aminobenzoate or ethyl *p*-aminobenzoate with $[\alpha\text{-}Mo_8O_{26}]^{4-}$ is more difficult, and the desired product is also obtained in moderate yield of ca. 40–50%. Apparently, the ester group is usually an electron-withdrawing group, which weakens the nucleophilic reactivity of amino groups in the ligands, therefore synthesis of the product is difficult. Through prolonging the reaction time and increasing the concentration of each raw material, the desired hybrids can now be obtained more easily and conveniently (see Scheme 1).

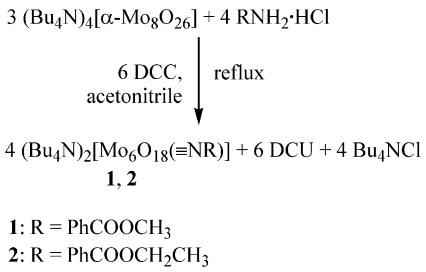

Scheme 1. Synthesis of hybrids of local anesthetic analogs and polyoxometalates (DCU stands for *N*,*N*′-dicyclohexylurea).

As was demonstrated previously,[28] the optimum reaction conditions such as the amount of each raw material and the reaction time can be obtained by monitoring the reaction system with TLC, UV/Vis, or ^{1}H NMR and a favorable routine was obtained and is given in the Exp. Section.

Both the two ester derivatives of hexamolybdate **1** and **2** are well soluble in most common organic solvents such as acetone, acetonitrile, *N*,*N*-dimethylformamide (DMF), and dimethyl sulfoxide (DMSO). However, from ESI mass spectroscopy, they are found to be unstable in neutral or basic solution. It was confirmed that Mo≡N triple bonds were frail and can be attacked by H_2O or OH^-, thus leading to the decomposition of the title molecules. They could decompose into $[Mo_6O_{19}]^{2-}$ or $[Mo_8O_{26}]^{4-}$, depending on the pOH value of the solution, and the ligand fragments correspondingly turned into the former organic ligand and released the local anesthetic analogs. In the process, organic ligands were first grafted onto hexamolybdate with the help of a DCC-catalyzed dehydration protocol. Then in the second step the inorganic–organic hybrid compounds decomposed to release the organic ligands under neutral or basic environments. Such properties could be applied to develop a novel controlled-release technology for drug delivery. Drugs could be first attached onto the surface of parent POMs and the resultant molecules delivered into the body of an organism. The molecules will then decompose and release the drugs. Their structures were determined by single-crystal X-ray diffraction analysis. Elemental analysis, ^{1}H NMR, IR, and UV/Vis were finally applied to confirm their structures and composition.

X-ray Structural Studies

The structures of hybrids **1** and **2** were determined by single-crystal X-ray diffraction analysis. A summary of X-ray crystallographic data for hybrids **1** and **2** is provided in Table 1. ORTEP representations of anions within **1** and **2** are given in Figure 1. Both of the structures show features of imido derivatives of hexamolybdates. For example, because of the so-called "*trans* influence," the central oxygen atom inside the cluster cage is drawn significantly closer to the imido-bearing Mo atom (the bond length of Mo1–O1, compared to that of Mo6–O1, is shorter by 0.133 Å in **1** or 0.126 Å in **2**). Compared to the parent hexamolybdate and other derivatives, the bond lengths of the five terminal oxo ligands of **1** and **2** do not vary significantly. In each of these mono-imido hexamolybdates, the arylimido group is bound in a terminal position at the hexamolybdate in a monodentate fashion, that is, it occupies a terminal site on the hexamolybdate cage. The short Mo–N bond lengths (1.713(9) Å in **1**, 1.723(9) Å in **2**) and the C1–N1–Mo1 bond angles [157.73(60)° in **1**, 173.42(83)° in **2**] are typical of organoimido groups bonded at an octahedral d^0 metal center and are consistent with a substantial degree of Mo≡N triple bond character. Similar with our previous research, the imido-bearing molybdenum atom demonstrates weaker electropositivity than other molybdenum atoms as one consequence of coordination with better electron-donating alkyl imido ligands, and therefore the bond lengths

of Moa–Ob (Ob is the bridge oxygen ligand) are longer than that of Mob–Ob. Another notable structural feature is that the long Mob–Ob and short Mob–Ob bond alternate in the equatorial and longitudinal (Mo)4(Ob)4 belt of these alkylimido derivatives.[29]

Table 1. Crystal data and structure refinement for compound **1** and **2**.

Compound	**2**	**1**
Empirical formula	$C_{41}H_8Mo_6N_3O_{20}$	$C_{40}H_{79}Mo_6N_3O_{20}$
Size [mm^3]	$0.23 \times 0.13 \times 0.04$	$0.20 \times 0.20 \times 0.08$
Formula weight	1511.73	1497.70
Crystal system	triclinic	monoclinic
Space group	$P\bar{1}$	$P2_1/n$
a [Å]	12.4260(11)	17.273(4)
b [Å]	12.9530(12)	15.530(3)
c [Å]	19.5278(19)	22.003(4)
α [°]	72.753(4)	90
β [°]	74.340(4)	106.21(3)
γ [°]	9.799(4)	90
V [Å^3]	2874.2(5)	5667(2)
Z	2	4
$D_{calc.}$ [g/cm^3]	1.747	1.755
Absorption coeff. [mm^{-1}]	1.338	1.356
F(000)	1520	3008
θ range [°]	1.66 to 25.00	3.10 to 25.00
Reflections collected	19579	43013
R(int)	0.0455	0.0848
GOF on F_2	1.021	1.030
Final R	0.0560	0.0576
Final R_w	0.1288	0.1315

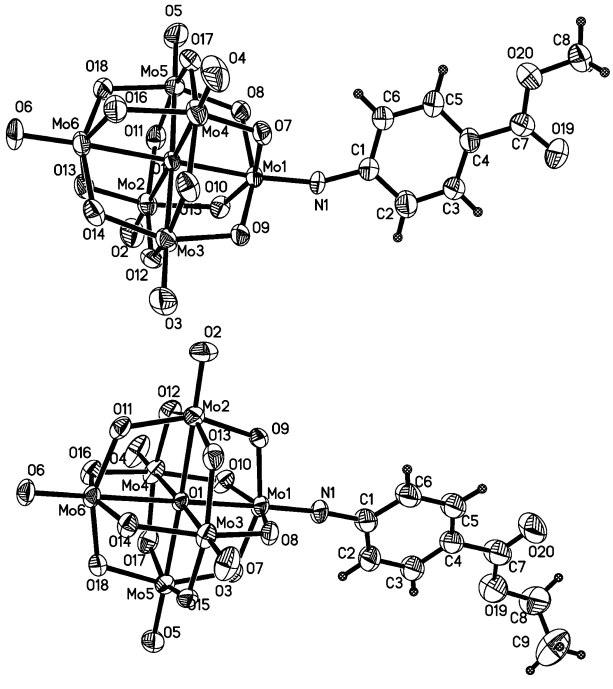

Figure 1. ORTEP drawings of the $[Mo_6O_{18}(\equiv NR)]^{2-}$ anions of **1** (top) and **2** (bottom).

Interestingly, hydrogen bonding plays an important role in the assembly of molecules in crystals of the two compounds. In derivative **1**, the methyl group of the ester was linked to the bridge oxygen of another anion through the C8–H···O17 hydrogen bond. And in this way, a dimer was formed (see Table 2 and Figure 2). Similarly, a dimer structure also exists in the crystal of compound **2**. However, the dimer was formed due to the hydrogen bonding between the terminal carbon atom of ethyl and the oxygen atom of the ester group in another anion (C9–H···O20, see Table 2 and Figure 3). And the dimers were further linked to form a one-dimensional chain due to the C8–H···O11 hydrogen bond (see Table 2, Figures 3 and 4). In the crystal of compound **2**, anions were first linked to form the dimers, which work as second building blocks, and the hydrogen bonds are linkers. Finally, the chain structure was obtained .

Table 2. Hydrogen bond lengths [Å] and bond angles [°].

D–H···A	d(D–H)	d(H···A)	d(D···A)	∠DHA
Compound **1**				
C(8)–H(8A)···O(17)[a]	0.96(5)	2.65(5)	3.029(5)	102(6)
Compound **2**				
C(9)–H(9A)···O(20)[b]	0.95(9)	2.57(5)	3.296(6)	139(1)
C(8)–H(8A)···O(11)[c]	0.96(8)	2.56(6)	3.322(6)	135(1)

[a] Symmetry codes: $-x + 1, -y, -z$. [b] $-x, -y + 2, -z$. [c] $x - 1, y + 1, z$.

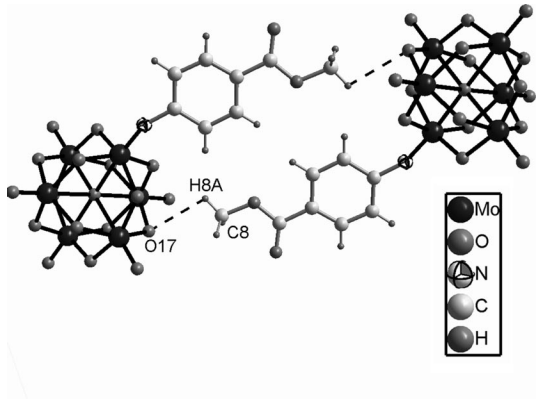

Figure 2. The dimer structure in the crystal of compound **1**.

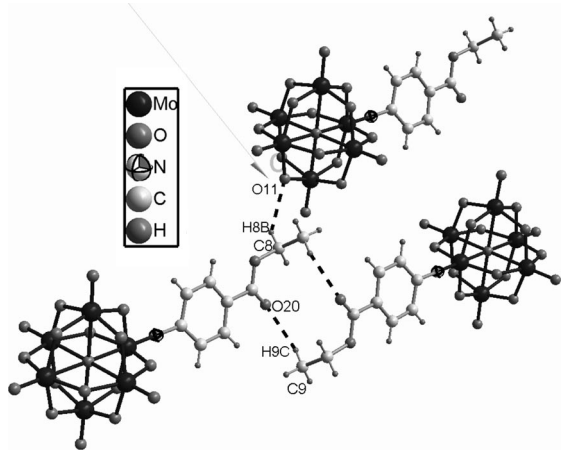

Figure 3. The dimer structure and hydrogen bonds in the crystal of compound **2**.

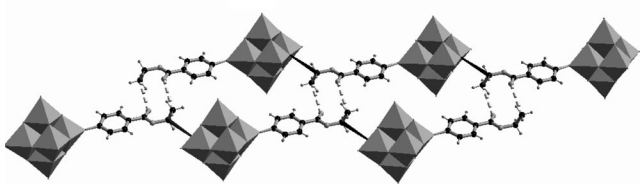

Figure 4. The chain structure of compound **2** (grey octahedron represents MoO_6; grey dot line represents C9–H···O20 hydrogen bond; black line represents C8–H···O11 hydrogen bond).

UV/Vis Spectroscopy

Figure 5 shows the UV/Vis absorption spectra of the tetrabutylammonium salt of $[Mo_6O_{19}]^{2-}$, $[\alpha\text{-}Mo_8O_{26}]^{4-}$, hybrids of compounds **1** and **2**. As demonstrated previously,[28] by comparing the different UV/Vis absorption spectra, it was indicated that the raw material $[(C_4H_9)_4N]_4[\alpha\text{-}Mo_8O_{26}]$ has changed into derivatives of $[(C_4H_9)_4N]_2[Mo_6O_{19}]$. The typical lowest energy electronic transition at 325 nm in $[Mo_6O_{19}]^{2-}$ was also bathochromically shifted by more than 23 nm and becomes considerably more intense in **1** (348 nm), and **2** (353 nm), indicating that the Mo–N π-bond is formed in these organoimido derivatives. In other words, there is a strong electronic interaction between the metal oxygen cluster and the organic conjugated ligands. The bathochromic shift on going from **1** (348 nm) to **2** (353 nm) is consistent with the conjugation effect of substituents in the imido ligands, resulting from the fact that the electron-donating effect of the ethylic group is stronger than that of the methyl group.

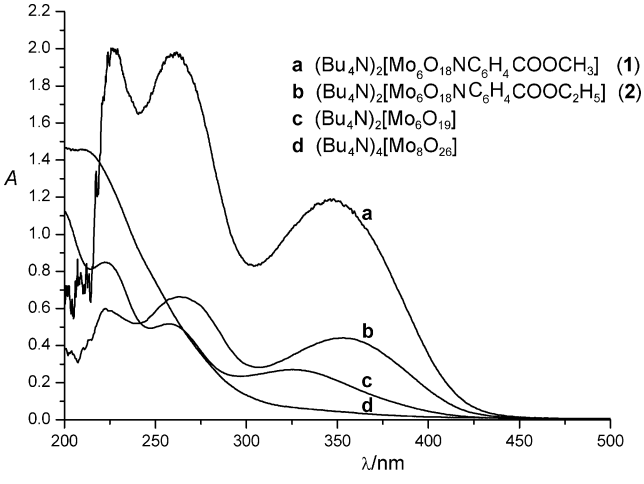

Figure 5. UV/Vis absorption spectra of $(Bu_4N)_2[Mo_6O_{19}]$, $(Bu_4N)_4[\alpha\text{-}Mo_8O_{26}]$, **1** and **2**.

NMR Spectroscopy

The ^1H NMR spectra (in $[D_6]$DSMO) of compound **1** or **2** shows clearly resolved signals, all of which can be unambiguously assigned. The integration of the peaks matches well with the assumed structures (see Figure 1). Compared to the ^1H NMR spectra of the corresponding free amine ligands, the protons of **1** or **2**, except for those in the tetrabutylammonium cation, all exhibit significantly downfield chemical shifts, indicating the much weaker shielding nature of the $[Mo_5O_{18}(Mo{\equiv}N{-})]^{2-}$ than the amino group. For example, the chemical shift of the proton in the benzene ring (δ = 8.01 or 7.30 in **1**, and δ = 8.02 or 7.31 in **2**) exhibits more significantly downfield shifts than that of the raw materials. In addition, the chemical shift of the proton in the methyl or ethyl of the ester group (δ = 3.85 in **1** and δ = 4.31 or 1.30 in **2**) also showed appreciable downfield shifts compared to the raw materials. By comparing the ^1H NMR spectra of compounds **1** and **2**, the chemical shifts of the proton in the benzene ring and the methyl or ethyl of the ester group implies the much stronger electron-withdrawing power of the $[Mo_5O_{18}(Mo{\equiv}N{-})]^{2-}$ and the carboxyl in **1** and **2**, which is in good agreement with the electronic character of their substituted groups in the benzene ring. Therefore, the ^1H NMR spectra can be used diagnostically for the formation of the desired hybrids.

IR Spectroscopy

The FT-IR spectra of the title compounds **1** and **2** are similar to each other, and resemble those of previously reported mono-organoimido derivatives.[7–12] All of them closely resemble that of the hexamolybdate parent. The very strong bands at 796, 956 cm^{-1} in **1** and 795, 953 cm^{-1} in **2**, represent the typical ν(Mo–O–Mo) and ν(Mo–O_t) vibrations, respectively. The band at around 976 cm^{-1} in the parent appeared as a shoulder of the 956 cm^{-1} band in **1** and 953 cm^{-1} in **2** and is tentatively assigned to the ν(Mo–N) vibration, which can also be used diagnostically for formation of the desired hybrids. Analogs of mono-alkylimido derivatives of hexamolybdate will also present similar FT-IR spectra characters. Other bands can be easily attributed to ν(C–H), ν(C–C) and ν(C=C). In addition, the very strong bands at 1719 cm^{-1} in **1** and 1713 cm^{-1} in **2**, represent the typical ν(C=O) vibration. The bands show slight shifts in relation to the different substituted group (CH_3 or C_2H_5), which is in good agreement with the electronic and conjugated character of the substituted groups.

Additionally, the two hybrids **1** and **2** were also confirmed by their ESI mass spectra, wherein three typical ion peaks with general formula $[(TBA)A]^-$, $[HA]^-$, and $[A]^{2-}$ (A = $[Mo_6O_{18}(NR)]^{2-}$) are presented in the negative-ion mode. The ESI-MS (*m*/*z*) values of 507, 1015, 1255 for **1** and 513, 1269 for **2**, are all in good agreement with the corresponding calculated values.

Conclusions

In summary, two local anesthetic analog derivatives of hexamolybdate bearing an electron-withdrawing ester group (R = *p*-$CH_3OOCC_6H_4$, *p*-$CH_3CH_2OOCC_6H_4$) have been prepared in high purity and moderate yields. Although the ester group is usually considered as an electron-withdrawing group, factually it presents the properties of an electron-donating group in the structures and UV/Vis spec-

tra. Such a feature is consistent with the conjugated effect of the ester group. Furthermore, by ^{1}H NMR, IR and ESI-MS studies, their character was also confirmed in other ways. In addition, the two compounds were found to be unstable in basic solution leading to release of the local anesthetic analogs. This property opens up another route to novel controlled-release technology for drug delivery and related studies may provide new possibilities in the development of pharmaceutical products.

Experimental Section

General: All syntheses and manipulations were performed in air, using ordinary organic synthetic apparatus and techniques. The starting material $(Bu_4N)_4[\alpha\text{-}Mo_8O_{26}]$ was conveniently prepared according to a reference procedure that has been presented in our previous papers.[28] Acetonitrile was dried by refluxing in the presence of CaH_2 and distilled prior to use. Other chemicals and solvents were obtained from commercial sources and were used as received without further purification. The elemental analysis was performed with a Vario EL (Elementar Analysensysteme GmbH). ^{1}H NMR spectra were recorded at 300 MHz and 298 K using a nuclear magnetic resonance spectrometer instrument (JOEL JNM-ECA300). The infrared spectrum was recorded within the 450–4000 cm^{-1} region on a Spectrum One FT-IR spectrometer (Perkin–Elmer) using KBr pellets. UV/Vis spectra were recorded with a UV-2100s UV/Visible Recording spectrophotometer (Shimadzu). Electrospray ionization mass spectrometry (ESI-MS) spectra were obtained with a Finnigan LCQ Deca XP Plus ion-trap mass spectrometer (San Jose, CA), and all experiments were carried out in the negative-ion mode. The complex solution was infused into the mass spectrometer at a flow rate of 2 mL min^{-1}. The electrospray source conditions were optimized to favor the detection of the non-covalent complexes (capillary voltage 33 V, capillary temperature 25 °C). In all experiments, the scanned mass range was set at 1000–2000 u. Data were collected and analyzed by using the Xcalibur software developed by ThermoFinnigan, and ten scans were averaged for each spectrum.

Synthesis of $(Bu_4N)_2[Mo_6O_{18}(\equiv NR)]$ (1, R = *p*-$CH_3OOCC_6H_4$): A typical synthetic routine for the hybrid of local anesthetic analogs and polyoxometalates bearing an electron-withdrawing ester group (R = *p*-$CH_3OOCC_6H_4$,**1**) is as follows: a mixture of $(Bu_4N)_4[\alpha\text{-}Mo_8O_{26}]$ (1.0 mmol), DCC (3.0 mmol), and methyl *p*-aminobenzoate hydrogen halide salts (2.0 mmol) was refluxed in anhydrous acetonitrile (10 mL) for about 12 h. When the mixture had dissolved completely in anhydrous acetonitrile at room temperature, the solution became achromatous, and then some white precipitates formed. About 5 min later, at a temperature of 80°C, the white precipitates dissolved again. With the reaction continuing, its color changed to red, and some white precipitates (*N*,*N*′-dicyclohexylurea) formed. After being cooled down to room temperature, filtration of the resulting dark red solution removed the white precipitates. While most of the acetonitrile evaporated out, the product precipitated from the filtrate as a salmon-pink crystalline solid. The product was collected by filtration, washed several times successively with EtOH and Et_2O, and then recrystallized twice from a mixed solution of acetone and EtOH (1:1). The product deposited as salmon pink crystals usually in about 40–50% yield. $C_{40}H_{79}Mo_6N_3O_{20}$ (1497.72): calcd. C 32.08, H 5.32, N 2.80; found C 32.26, H 5.33, N 2.72. ^{1}H NMR (300 MHz, [D$_6$]DSMO, 298 K): δ = 0.93 (t, $^3J_{H\text{-}H}$ = 7.2 Hz, 24 H, CH_3, $[Bu_4N]^+$), 1.31 (m, 16 H, CH_2, $[Bu_4N]^+$), 1.57 (m, 16 H, CH_2, $[Bu_4N]^+$), 3.18 (t, $^3J_{H\text{-}H}$ = 8.40 Hz, 16 H, NCH_2, $[Bu_4N]^+$), 3.85 (s, 3 H, CH_3, $ArCOOCH_3$), 7.30 (d, $^3J_{H\text{-}H}$ = 14.0 Hz, 2 H, *m*-H-Ar-NMo), 8.01 (d, $^3J_{H\text{-}H}$ = 14.0 Hz, 2 H, *o*-H-ArNMo) ppm. IR (KBr pellet, major absorbances): $\tilde{\nu}$ = 2962, 2873, 1719, 1591, 1481, 1433, 1379, 1323, 1269, 1164, 1114, 956 (shoulder at 976), 878, 796, 596 cm^{-1}. UV/Vis (MeCN): λ_{max} (ε, $M^{-1}cm^{-1}$) = 226 (5.8×10^4), 261 (5.7×10^4), 353 (3.5×10^4) nm. Single crystals used for X-ray diffraction were obtained by diffusion of diethyl ether into a solution of hybrid **1** in acetone.

Synthesis of $(Bu_4N)_2[Mo_6O_{18}(\equiv NR)]$ (2, R = *p*-$CH_3CH_2OOCC_6H_4$): Hybrid **2** was synthesized using the same reaction and work up procedure as that of **1** (52%). $C_{41}H_{81}Mo_6N_3O_{20}$ (1511.74): calcd. C 32.58, H 5.40, N 2.78; found C 31.00, H 5.37, N 2.43. ^{1}H NMR (300 MHz, [D$_6$]DSMO, 298 K): δ = 0.94 (t, $^3J_{H\text{-}H}$ = 7.20 Hz, 24 H, CH_3, $[Bu_4N]^+$), 1.30 (t, $^3J_{H\text{-}H}$ = 7.5 Hz, 3 H, CH_3, $ArCOOCH_2CH_3$), 1.31 (m, 16 H, CH_2, $[Bu_4N]^+$), 1.56 (m, 16 H, CH_2, $[Bu_4N]^+$), 3.17 (t, $^3J_{H\text{-}H}$ = 8.4 Hz, 16 H, NCH_2, $[Bu_4N]^+$), 4.31 (q, $^3J_{H\text{-}H}$ = 7.5 Hz, 2 H, CH_2, $ArCOOCH_2CH_3$), 7.31 (d, $^3J_{H\text{-}H}$ = 14.0 Hz, 2 H, *m*-H-Ar-NMo), 8.02 (d, $^3J_{H\text{-}H}$ = 14.0 Hz, 2 H, *o*-H-ArNMo) ppm. IR (KBr pellet, major absorbances): $\tilde{\nu}$ = 2962, 2873, 1713, 1592, 1470, 1380, 1337, 1271, 1163, 1106, 953 (shoulder at 976), 878, 795, 597 cm^{-1}. UV/Vis (MeCN): λ_{max} (ε, $M^{-1}cm^{-1}$) = 223 (3.7×10^4), 264 (4.2×10^4), 348 (3.2×10^4) nm. Single crystals used for X-ray diffraction were obtained by diffusion of diethyl ether into a solution of hybrid **2** in acetone.

X-ray Crystallographic Structural Determinations: Summaries of crystal data, data collection, and refinement parameters are given in Table 1. A suitable single crystal having approximate dimensions $0.23\times0.13\times0.04$ mm^3 (for **1**) or $0.2\times0.2\times0.08$ mm^3 (for **2**) was mounted on a glass fiber. All measurements were made with a Rigaku R-AXIS RAPID imaging plate diffractometer. Data collection was performed at 293 K by using graphite-monochromated Mo-K_α radiation (λ = 0.71073 Å). Absorption corrections were applied by correlation of symmetry-equivalent reflections using the ABSCOR program.[30] Data reduction was performed by teXsan for Windows version 1.06.[31] Subsequent calculations were carried out using the SHELXTL version 5.10 program.[32] Structures were solved by direct methods. Refinements were performed by full-matrix least-squares analysis. The non-hydrogen atoms were refined anisotropically. Hydrogen atoms were included at their calculated positions but not refined.

Acknowledgments

This work is sponsored by the National Natural Science Foundation of China (Grants No. 20871073 and 20373001), and Beijing Forestry University Young Scientist Fund.

[1] M. T. Pope, A. Müller, *Angew. Chem. Int. Ed. Engl.* **1991**, *30*, 34–48.
[2] a) M. J. Morris, *Coord. Chem. Rev.* **1995**, *146*, 43–97; b) M. J. Morris, *Coord. Chem. Rev.* **1996**, *147*, 309–358.
[3] J. T. Rhule, C. L. Hill, D. A. Judd, R. F. Schinazi, *Chem. Rev.* **1998**, *98*, 327–357.
[4] A. Müller, H. Reuter, S. Dillinger, *Angew. Chem. Int. Ed. Engl.* **1995**, *34*, 2328–2361.
[5] M. T. Pope, *Heteropoly and Isopolyoxometalates*, Springer, New York, **1995**.
[6] T. Liu, E. Diemann, H. Li, A. W. M. Dress, A. Müller, *Nature* **2003**, *426*, 59–62.
[7] P. Gouzerh, A. Proust, *Chem. Rev.* **1998**, *98*, 77–111.
[8] A. Proust, R. Thouveout, P. Gouzerh, *Chem. Commun.* **2008**, 1837–1852.

[9] C. Sun, S. Liu, D. Liang, K. Shao, Y. Ren, Z. Su, *J. Am. Chem. Soc.* **2009**, *131*, 1883–1888.
[10] J. W. Han, C. L. Hill, *J. Am. Chem. Soc.* **2007**, *129*, 15094–15095.
[11] L. Yan, M. Jin, J. Zhuang, C. Liu, Z. Su, C. Sun, *J. Phys. Chem. A* **2008**, *112*, 9919–9923.
[12] Y. Sun, N. McMillan, D. Long, S. Kane, J. Malm, M. O. Riehle, C. P. Pradeep, N. Gadegaard, L. Cronin, *J. Am. Chem. Soc.* **2009**, *131*, 1340–1341.
[13] J. Zhang, Y. Song, L. Cronin, T. Liu, *J. Am. Chem. Soc.* **2008**, *130*, 14408–14409.
[14] Y. Song, D. Long, D. L. Cronin, *Angew. Chem. Int. Ed.* **2007**, *46*, 3900–3904.
[15] Y. Song, N. McMillan, D. Long, J. Thiel, Y. Ding, H. Chen, N. Gadegaard, L. Cronin, *Chem. Eur. J.* **2008**, *14*, 2349–2354.
[16] B. Hasenknopf, R. Delmont, P. Herson, P. Gouzerh, *Eur. J. Inorg. Chem.* **2002**, 1081–1087.
[17] P. R. Marcoux, B. Hasenknopf, J. Vaissermann, P. Gouzerh, *Eur. J. Inorg. Chem.* **2003**, 2406–2412.
[18] C. F. Pradeep, D. Long, G. N. Newton, Y. Song, L. Cronin, *Angew. Chem. Int. Ed.* **2008**, *47*, 4388–4391.
[19] A. R. Moore, H. Kwen, A. M. Beatty, E. A. Maatta, *Chem. Commun.* **2000**, 1793–1794.
[20] M. Lu, Y. Wei, B. Xu, C. F. Cheung, Z. Peng, *Angew. Chem. Int. Ed.* **2002**, *41*, 1566–1568.
[21] Y. Zhu, L. Wang, J. Hao, P. Yin, J. Zhang, Q. Li, L. Zhu, Y. Wei, *Chem. Eur. J.* **2009**, *15*, 3076–3080.
[22] L. Zhu, Y. Zhu, X. Meng, J. Hao, Q. Li, Y. Wei, Y. Lin, *Chem. Eur. J.* **2008**, *14*, 10923–10927.
[23] L. Wang, L. Zhu, P. Yin, W. Fu, J. Chen, J. Hao, F. Xiao, C. Lv, J. Zhang, L. Shi, Q. Li, Y. Wei, *Inorg. Chem.* **2009**, *48*, 9222–9235.
[24] S. Xue, A. Chai, Y. Wei, C. Xiang, W. Bian, J. Shen, *J. Mol. Struct.* **2008**, *888*, 300–306.
[25] S. Xue, C. Xiang, Y. Wei, Z. Tao, A. Chai, W. Bian, Z. Xu, *Cryst. Growth Des.* **2008**, *8*, 2437–2443.
[26] Q. Xin, R. Xu, Z. Zhou, *Fundamental Organic Chemistry*, Advance Education Press, **1985**, vol. 2.
[27] a) K. Fifa, *J. Pharm. Pharmacol.* **2009**, *61*, 121–124; b) C. G. Haining, *J. Pharm. Pharmacol.* **1960**, *12*, 641–647; c) A. C. Schmidt, *Int. J. Pharm.* **2005**, *298*, 186–197; d) http://www.drugs.com/mtm/benzocaine-topical.html.
[28] a) Y. Wei, B. Xu, C. L. Barnes, Z. H. Peng, *J. Am. Chem. Soc.* **2001**, *123*, 4083–4084; b) P. Wu, Q. Li, N. Ge, Y. Wei, Y. Wang, P. Wang, H. Guo, *Eur. J. Inorg. Chem.* **2004**, 2819–2822.
[29] a) T. M. Che, V. W. Day, L. C. Francesconi, M. F. Fredrich, W. G. Klemperer, *Inorg. Chem.* **1985**, *24*, 4055–4062; b) J. Fuchs, W. Freiwald, H. Hartl, *Acta Crystallogr., Sect. B* **1978**, *34*, 1764–1770.
[30] T. Higashi, *ABSCOR* - Empirical Absorption Correction based on Fourier Series Approximation, Rigaku Corporation, Tokyo, Japan, **1995**.
[31] Molecular Structure Corporation, *TEXSAN MSC*, 3200 Research Forest Drive, The Woodlands, TX 77381, USA, **1997**–**1999**.
[32] G. M. Sheldrick, *SHELXTL version 5.10*, Structure Determination Software Suite, Bruker AXS, Madison, Wisconsin, USA, **1998**.

Received: June 28, 2009
Published Online: October 12, 2009

